

# Methylpyrazole-Capped Two-Dimensional Supramolecular M(II) (M = Mn, Ni, Co) Assemblies Constructed by Covalent and Noncovalent Interactions: Uncommon Coordination Modes of Methylpyrazoles and Magnetic Properties

Da Hye Choi,<sup>†</sup> Jung Hee Yoon,<sup>†</sup> Jeong Hak Lim,<sup>†</sup> Hyoung Chan Kim,<sup>‡</sup> and Chang Seop Hong<sup>\*†</sup>

Department of Chemistry and Center for Electro- and Photo-Responsive Molecules, Korea University, Seoul 136-701, Korea, and Systems Research Team, Research & Development Division, Nuclear Fusion Research Center, Daejeon 305-333, Korea

Received March 14, 2006

Two mononuclear complexes [Mn(5-methylpyrazole)<sub>4</sub>(N<sub>3</sub>)<sub>2</sub>] (**1**) and [Ni(5-methylpyrazole)<sub>4</sub>(N<sub>3</sub>)<sub>2</sub>] (**2**), as well as a novel one-dimensional coordination polymer [Co(3-methylpyrazole)<sub>2</sub>(5-methylpyrazole)<sub>2</sub>(tp)]<sub>n</sub> (**3**) (tp = terephthalate), were characterized. The isostructural complexes, **1** and **2**, display two-dimensional supramolecular networks formed by hydrogen bonds between the N–H groups of 5-methylpyrazoles and the end N atoms of the azide ligands and additional face-to-face  $\pi$ – $\pi$  interactions of the 5-methylpyrazoles. For **3**, tp-bridged one-dimensional chains assisted by intrachain hydrogen bonds among the N–H groups of methylpyrazoles and carboxylate oxygens are connected with the help of interchain C–H...O hydrogen bonds, leading to a two-dimensional structure. The intra- and interchain hydrogen bonds account for the coexistence of two unique coordination forms (5-methylpyrazole and 3-methylpyrazole) of methylpyrazoles in the same coordination sphere. Weak antiferromagnetic interactions coupled with the spin–orbit coupling effect are operative in **3** through the tp ligands.

## Introduction

The design of coordination polymers has been extensively explored recently because of promising applications in molecule-based magnetic materials and metal–organic frameworks.<sup>1</sup> To this end, the terephthalate (= tp) ligand is one of the most frequently utilized spacers, whose diverse binding modes and facile intermolecular interactions (hydrogen bonds, face-to-face  $\pi$ – $\pi$ , and edge-to-face CH– $\pi$  interactions) are good sources for the formation of multidimensional supramolecular entities.<sup>2</sup> Another essential ingredient to control molecular structures is capping ligands that can fill up coordination sites around metal centers. Among them, pyrazoles with binding capabilities arising from the N atom for coordination to a metal atom, the N–H group for hydrogen bonding, and the planar aromatic ring for other intermolecular forces have been successfully employed for the

construction of supramolecular assemblies with various structures.<sup>2,3</sup> For instance, the use of 3(5)-methylpyrazole is able to produce one- and three-dimensional coordination polymers consisting of exclusively 5-methylpyrazole as a binding mode.<sup>3</sup>

In coordination chemistry, bridging and capping ligands including simple well-known units of SCN<sup>−</sup>, NO<sub>2</sub><sup>−</sup>, CN<sup>−</sup>, and NO tend to be subject to linkage isomerism induced by external stimuli such as electrochemistry, pH, light, and pressure.<sup>4</sup> Interestingly, for the thiocyanate ion, the coexistence of two coordination modes of the SCN group in M–(SCN)(NCS), which occurs in an identical coordination

\* To whom correspondence should be addressed. E-mail: cshong@korea.ac.kr.

<sup>†</sup> Korea University.

<sup>‡</sup> Nuclear Fusion Research Center.

(1) (a) Lescouëzec, R.; Toma, L. M.; Vaissermann, J.; Verdager, M.; Delgado, F. S.; Ruiz-Pérez, C.; Lloret, F.; Julve, M. *Coord. Chem. Rev.* **2005**, *249*, 2691. (b) Kitagawa, S.; Kitaura, R.; Noro, S.-i. *Angew. Chem., Int. Ed.* **2004**, *43*, 2334.

(2) (a) Hong, C. S.; Yoon, J. H.; Lim, J. H.; Ko, H. H. *Eur. J. Inorg. Chem.* **2005**, 4818. (b) Hong, C. S.; Do, Y. *Inorg. Chem.* **1998**, *37*, 4470. (c) Li, H.; Eddaoudi, M.; O'Keeffe, M.; Yaghi, O. M. *Nature* **1999**, *402*, 276. (d) Rowsell, J. L. C.; Yaghi, O. M. *Angew. Chem., Int. Ed.* **2005**, *44*, 4670. (e) James, S. L. *Chem. Soc. Rev.* **2003**, *32*, 276. (f) Go, Y.; Wang, X.; Anokhina, E. V.; Jacobson, A. J. *Inorg. Chem.* **2004**, *43*, 5360. (g) Li, L.; Liu, Z.; Turner, S. S.; Liao, D.; Jiang, Z.; Yan, S. *Eur. J. Inorg. Chem.* **2003**, 62.

(3) (a) Hong, C. S.; Do, Y. *Inorg. Chem.* **1997**, *36*, 5684. (b) Hong, C. S.; Koo, J.-e.; Son, S.-K.; Lee, Y. S.; Kim, Y.-S.; Do, Y. *Chem.–Eur. J.* **2001**, *7*, 4243. (c) Hong, C. S.; Do, Y. *Angew. Chem., Int. Ed.* **1999**, *38*, 193. (d) Hong, C. S.; You, Y. S. *Polyhedron* **2004**, *23*, 3043.

sphere, was characterized structurally.<sup>5</sup> However, such examples are very scarce to date, and hence, to get insight into how to stabilize two coordination forms of capping ligands concurrently, suitable systems have been sought.

Herein, we report the synthesis and crystal structures of two monomers, [Mn(5-methylpyrazole)<sub>4</sub>(N<sub>3</sub>)<sub>2</sub>] (**1**) and [Ni(5-methylpyrazole)<sub>4</sub>(N<sub>3</sub>)<sub>2</sub>] (**2**), which are extended to two-dimensional frameworks associated with hydrogen bonds and  $\pi$ - $\pi$  interactions, and a novel Co(II) compound [Co(3-methylpyrazole)<sub>2</sub>(5-methylpyrazole)<sub>2</sub>(tp)]<sub>n</sub> (**3**) bridged by tp and hydrogen bonds. It is worth noting that compounds **1** and **2** show the exclusive coordination mode of 5-methylpyrazole, whereas the Co metal center in **3** accommodates two binding types of the capping ligand, 5-methylpyrazole and 3-methylpyrazole, in the coordination sphere at the same time, which is a very unique example of the linkage isomers.<sup>4,5</sup> Magnetic studies on **3** demonstrate that weak antiferromagnetic interactions between Co spins exist through the tp linkage, together with the spin-orbit coupling effect.

## Experimental Section

**Reagent.** All chemicals and solvents in the synthesis were of reagent grade and were used as received. All manipulations were performed under aerobic conditions.

**Synthesis. Caution:** Perchlorate salts of metal compounds with organic ligands are potentially explosive. Only small amounts of material should be handled.

**[Mn(5-methylpyrazole)<sub>4</sub>(N<sub>3</sub>)<sub>2</sub>] (**1**).** A 10 mL aqueous solution of manganese(II) perchlorate hexahydrate (1.0 mmol) was treated with 3(5)-methylpyrazole (4.0 mmol) with stirring. A 10 mL aqueous solution of sodium azide (2.0 mmol) was added to the resulting solution. The filtrate was allowed to stand undisturbed in the refrigerator, giving colorless crystals in a yield of 17%. Anal. Calcd for C<sub>16</sub>H<sub>24</sub>MnN<sub>14</sub>: C, 41.12; H, 5.18; N, 41.95. Found: C, 41.09; H, 5.20; N, 41.82.

**[Ni(5-methylpyrazole)<sub>4</sub>(N<sub>3</sub>)<sub>2</sub>] (**2**).** A 10 mL aqueous solution of nickel(II) acetate tetrahydrate (1.0 mmol) was treated with 3(5)-methylpyrazole (4.0 mmol) with stirring. A 10 mL aqueous solution of sodium azide (2.0 mmol) was added to the resulting solution, giving sky blue precipitate which was collected by filtration, washed with water, and dried in air. The filtrate was allowed to stand undisturbed, and blue crystals were deposited. Yield: 80%. Anal. Calcd for C<sub>16</sub>H<sub>24</sub>N<sub>14</sub>Ni: C, 40.79; H, 5.13; N, 41.62. Found: C, 40.67; H, 5.18; N, 42.03.

**[Co(3-methylpyrazole)<sub>2</sub>(5-methylpyrazole)<sub>2</sub>(tp)]<sub>n</sub> (**3**).** Compound **3** was obtained by dropwise addition of 3(5)-methylpyrazole (2.0 mmol) to an aqueous solution of cobalt(II) perchlorate hexahydrate (0.50 mmol). The resulting mixture was treated with dipotassium tp (0.50 mmol) in water with 10 min of stirring. Slow evaporation of the filtrate gave pink crystals **3** in a 45% yield. Anal. Calcd for C<sub>24</sub>H<sub>28</sub>CoN<sub>8</sub>O<sub>4</sub>: C, 52.27; H, 5.12; N, 20.32. Found: C, 52.29; H, 5.11; N, 20.21.

**Table 1.** Crystallographic Data for **1**, **2**, and **3**

	<b>1</b>	<b>2</b>	<b>3</b>
formula	C <sub>8</sub> H <sub>12</sub> Mn <sub>0.5</sub> N <sub>7</sub>	C <sub>8</sub> H <sub>12</sub> N <sub>7</sub> Ni <sub>0.5</sub>	C <sub>12</sub> H <sub>14</sub> Co <sub>0.5</sub> N <sub>4</sub> O <sub>2</sub>
fw	233.72	235.60	275.74
cryst syst	monoclinic	monoclinic	monoclinic
space group	<i>P</i> 2 <sub>1</sub> / <i>c</i>	<i>P</i> 2 <sub>1</sub> / <i>c</i>	<i>C</i> 2/ <i>c</i>
<i>a</i> (Å)	8.8530(10)	9.0340(17)	11.4804(2)
<i>b</i> (Å)	9.0560(10)	9.0935(7)	13.3369(2)
<i>c</i> (Å)	14.884(2)	14.314(3)	16.8693(3)
$\alpha$ (deg)	90	90	90
$\beta$ (deg)	104.67(2)	107.954(17)	94.5930(10)
$\gamma$ (deg)	90	90	90
<i>V</i> (Å <sup>3</sup> )	1154.4(2)	1118.7(3)	2574.61(7)
<i>Z</i>	4	4	8
<i>d</i> <sub>calcd</sub> (g cm <sup>-3</sup> )	1.345	1.399	1.423
$\mu$ (mm <sup>-1</sup> )	0.605	0.902	0.713
<i>F</i> (000)	486	492	1148
$\theta$ range (deg)	2.38–24.98	2.37–24.99	2.35–28.30
unique reflns	1730	1898	3196
no. of params	124	124	195
R1 <sup>a</sup> [ <i>I</i> > 2 $\sigma$ ( <i>I</i> )]	0.0369	0.0551	0.0452
wR2 <sup>b</sup> [ <i>I</i> > 2 $\sigma$ ( <i>I</i> )]	0.0551	0.1595	0.1153

$$^a R1 = \sum ||F_o| - |F_c|| / \sum |F_c|. \quad ^b wR2 = [\sum w(F_o^2 - F_c^2)^2 / \sum w(F_o^2)^2]^{1/2}.$$

**Physical Measurements.** Elemental analyses for C, H, and N were performed at the Elemental Analysis Service Center of Sogang University. Infrared spectra were obtained from KBr pellets with a Bomem MB-104 spectrometer. Magnetic susceptibility data for **3** were carried out at 0.1 T using a Quantum Design MPMS-7 SQUID susceptometer. Diamagnetic corrections of **3** were estimated from Pascal's tables.

**Crystallographic Structure Determination.** X-ray data were collected on an Enraf-Nonius CAD4TSB diffractometer for **1** and **2** and a Bruker SMART APEXII diffractometer for **3** equipped with graphite-monochromated Mo K $\alpha$  radiation ( $\lambda = 0.71073$  Å). The reflection data were corrected for Lorentz and polarization factors. The structures were solved by direct methods and refined by full-matrix least-squares analysis using anisotropic thermal parameters for non-hydrogen atoms with the SHELXTL program.<sup>6</sup> The hydrogens on the aromatic rings of the methylpyrazoles for **3** were refined isotropically. All hydrogen atoms except for the aforementioned hydrogens were calculated at idealized positions and refined with the riding models. Crystallographic data and the details of data collection are listed in Table 1.

## Results and Discussion

**Synthesis and Characterizations.** The treatment of M(II) ions (M = Mn, Ni) with 3(5)-methylpyrazole in the presence of sodium azide gave the stable compounds **1** and **2**. The binding pattern of methylpyrazoles to metal ions is evident from the IR spectra where the single broad N–H bands centered at 3318 (**1**) and 3297 cm<sup>-1</sup> (**2**) are observed, suggesting the existence of one type of coordination mode. The formation of the mononuclear compounds **1** and **2** can be favored by a bunch of hydrogen bonds of the N–H groups in methylpyrazoles as ascertained by the broad IR signals of the N–H vibrations and crystal structures described below. For **3**, a stoichiometric reaction of Co(ClO<sub>4</sub>)<sub>2</sub>·6H<sub>2</sub>O, 3(5)-methylpyrazole, and K<sub>2</sub>tp in water produced pink crystals. In the IR spectrum, the strong bands spanning from 3103 to 3185 cm<sup>-1</sup> with a broad background are typical of the

(4) (a) Lee, J.; Kovalevsky, A. Y.; Novozhilova, I. V.; Bagley, K. A.; Coppens, P.; Richter-Addo, G. B. *J. Am. Chem. Soc.* **2004**, *126*, 7180. (b) Coronado, E.; Giménez-López, M. C.; Levchenko, G.; Romero, F. M.; García-Baonza, V.; Milner, A.; Paz-Pasternak, M. *J. Am. Chem. Soc.* **2005**, *127*, 4580. (c) Johansson, O.; Lomoth, R.; *Chem. Commun.* **2005**, 1578. (d) Sisley, M. J.; McDonald, R.; Jordan R. B. *Inorg. Chem.* **2004**, *43*, 5339. (e) Kovalevsky, A. Yu.; King, G.; Bagley, K. A.; Coppens, P. *Chem.—Eur. J.* **2005**, *11*, 7254.  
(5) Kishi, S.; Kato, M. *Inorg. Chem.* **2003**, *42*, 8728.

(6) Sheldrick, G. M. *SHELXTL*, version 5; Bruker AXS: Madison, WI, 1995.

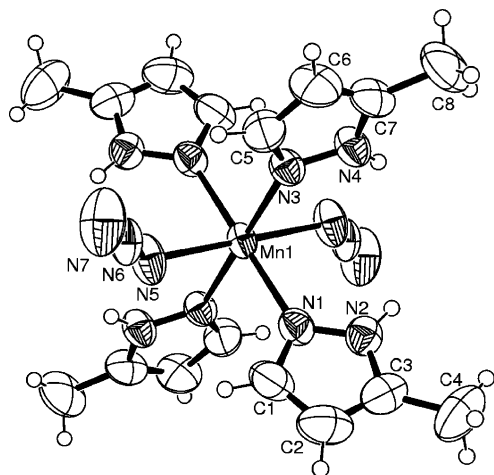


Figure 1. ORTEP representation of **1** showing the atom-labeling scheme.

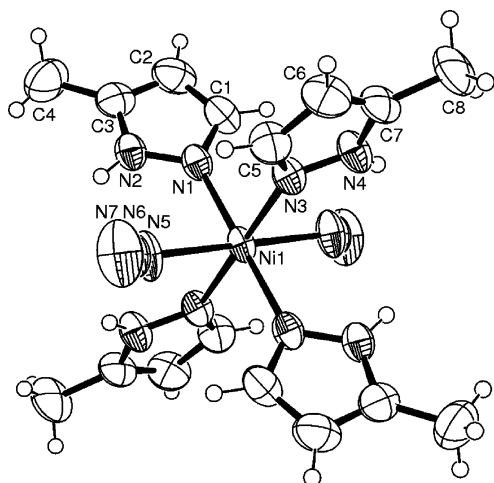


Figure 2. ORTEP representation of **2** showing the atom-labeling scheme.

presence of hydrogen-bonded N–H groups. Unlike the IR spectra in **1** and **2**, the multiple peaks in the NH stretching regime indicate that the coordination pattern of 3(5)-methylpyrazole to a metal ion is not identical but rather complicated, implying the coexistence of different binding modes of methylpyrazoles. The differences ( $\Delta$ ) between antisymmetric stretching  $\nu_a(\text{CO}_2^-)$  and symmetric frequency  $\nu_s(\text{CO}_2^-)$  range from 179 to 183  $\text{cm}^{-1}$ . The calculated  $\Delta$  values, which are comparable with the reference value (170  $\text{cm}^{-1}$ ) of dipotassium tp, support the idea that the binding mode of the carboxylate group of tp appears to be bridging via coordination and hydrogen bonding,<sup>7</sup> which is confirmed by X-ray analysis.

**Description of the Structures.**  $[\text{M}(\text{5-methylpyrazole})_4(\text{N}_3)_2]$ . The molecular views of  $\text{M} = \text{Mn}$  (**1**) and  $\text{Ni}$  (**2**) are represented in Figures 1 and 2 with the atom-labeling schemes. They crystallize in monoclinic crystal systems with the space group  $P2_1/c$  and are isostructural to each other. The overall structural features for **1** and **2** are almost identical; therefore the molecular structures of **1** are described

Table 2. Bond Lengths (Å) and Angles (deg) for **1**

Mn(1)–N(5)	2.210(2)	Mn(1)–N(1)	2.264(3)
Mn(1)–N(3)	2.2644		
N(5)–Mn(1)–N(1)	92.01(11)	N(5)–Mn(1)–N(3)	94.85(7)
N(1)–Mn(1)–N(3)	89.56(6)	N(6)–N(5)–Mn(1)	133.0(2)
C(1)–N(1)–Mn(1)	129.4(2)	N(2)–N(1)–Mn(1)	126.67(19)
C(5)–N(3)–Mn(1)	135.28(16)	N(4)–N(3)–Mn(1)	121.0

Table 3. Bond Lengths (Å) and Angles (deg) for **2**

Ni(1)–N(1)	2.105(2)	Ni(1)–N(5)	2.121(3)
Ni(1)–N(3)	2.1250		
N(1)–Ni(1)–N(5)	87.74(12)	N(1)–Ni(1)–N(3)	90.35(6)
N(5)–Ni(1)–N(3)	93.74(8)	N(6)–N(5)–Ni(1)	130.2(2)
C(1)–N(1)–Ni(1)	132.4(2)	N(2)–N(1)–Ni(1)	123.00(18)
C(5)–N(3)–Ni(1)	135.80(16)	N(4)–N(3)–Ni(1)	119.7

in detail. Selected bond lengths and angles are summarized in Tables 2 and 3. The M atom with an inversion center lies in a distorted octahedral environment consisting of four nitrogen atoms of the 5-methylpyrazole ligands and two axial nitrogen atoms of the azide ligands ( $\text{Mn–N (av)} = 2.25$  Å and  $\text{Ni–N (av)} = 2.12(1)$  Å). The  $\text{M–N5–N6}$  angle is  $133.0(2)^\circ$  for **1** and  $130.2(2)^\circ$  for **2**.

Hydrogen bonds are formed between the end N atoms of azide ligands and the N–H groups of 5-methylpyrazoles, as shown in Figure 3 and Table 4. The minor structural disparity between **1** and **2** is that all the N–H moieties of 5-methylpyrazoles in **2** participate in hydrogen bonding to the two end N atoms ( $\text{N2}\cdots\text{N7a} = 2.988$  Å,  $a = -x + 2, y + 1/2, -z + 3/2$ ;  $\text{N2}\cdots\text{N5} = 2.970$  Å;  $\text{N4}\cdots\text{N5b} = 2.817$  Å,  $b = -x + 2, -y, -z + 2$ ;  $\text{N4}\cdots\text{N7c} = 3.170$  Å,  $c = x, -y - 1/2, z + 1/2$ ) concurrently, while the N2–H2 group of 5-methylpyrazole in **1** is hydrogen-bonded only to the terminal N atom (N7) of the azide ligand ( $\text{N2}\cdots\text{N7a} = 2.981$  Å,  $a = x, -y + 1/2, z - 1/2$ ;  $\text{N4}\cdots\text{N7a} = 3.056$  Å;  $\text{N4}\cdots\text{N5b} = 2.978$  Å,  $b = -x + 2, -y + 1, -z + 1$ ). The shortest intermolecular distance of  $\text{M}\cdots\text{M}$  via the multiple hydrogen bonds is 8.711 Å for **1** and 8.479 Å for **2**. Interestingly, the N3-containing 5-methylpyrazoles are stacked through intermolecular  $\pi$ – $\pi$  interactions, and their distances are in the range of 3.712–4.086 Å for **1** and 3.753–4.228 Å for **2**. The  $\text{Mn}\cdots\text{Mn}$  separation along the contacts is similar, corresponding to 9.056 Å for **1** and 9.094 Å for **2**. The noncovalent interactions in **1** and **2** play a crucial role in stabilizing the coordination mode of 5-methylpyrazole, leading to the formation of two-dimensional supramolecular entities. The layers are packed in a corrugated fashion and the methyl groups of 5-methylpyrazoles are located outside of the layer (Figure S1).

$[\text{Co}(\text{3-methylpyrazole})_2(\text{5-methylpyrazole})_2(\text{tp})]_n$  (**3**). An ORTEP diagram of **3** showing the atom-labeling scheme is illustrated in Figure 4. Selected bond lengths and angles are given in Table 5. The Co atom adopts a distorted octahedral geometry composed of four nitrogen atoms of four methylpyrazoles and two oxygens of tp ligands. It deserves to be noted that, as expected from the IR spectrum, there are two binding types of methylpyrazoles, depending on the positions of coordination sites, such as 5-methylpyrazole and 3-methylpyrazole, which are rare cases of the linkage isomers.<sup>4,5</sup> The occurrence of the 3-methylpyrazole coordination mode

(7) Nakamoto, K. *Infrared and Raman Spectra of Inorganic and Coordination Compounds: Part B: Applications in Coordination, Organometallic, and Bioinorganic Chemistry*, 5th ed.; John Wiley & Sons: New York, 1997.

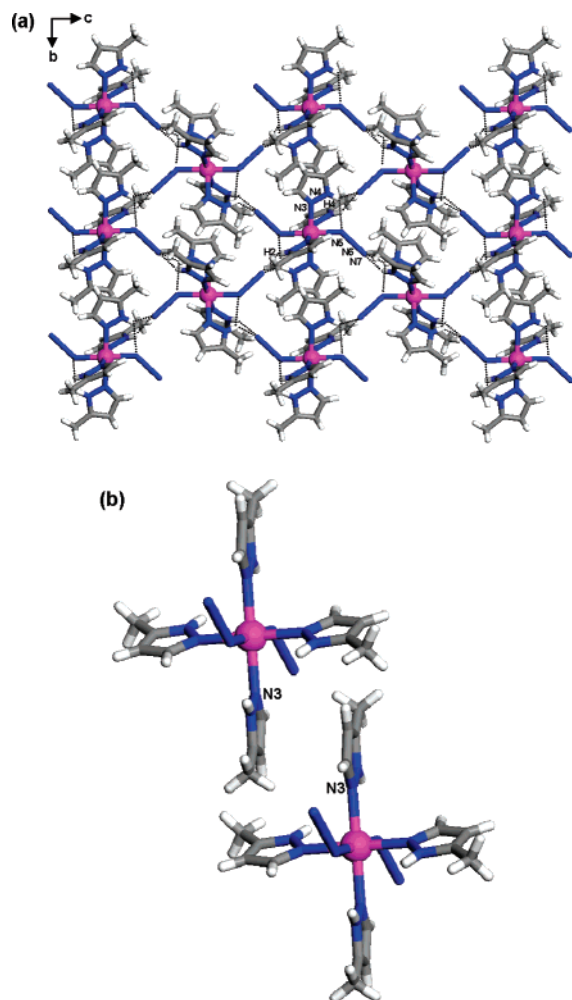


**Figure 3.** Molecular views of **1** with (a) an extended two-dimensional sheet constructed by hydrogen bonds (dotted lines) between end N atoms of azide ligands and the N–H groups of 5-methylpyrazoles and (b)  $\pi$ – $\pi$  interactions between the N3-containing pyrazole rings (C, gray; N, blue; Mn, pink).

**Table 4.** Hydrogen Bonds for **1**–**3** (Å and deg)

D–H···A	<i>d</i> (D–H)	<i>d</i> (H···A)	<i>d</i> (D···A)	$\angle$ (D–H···A)
<b>1<sup>a</sup></b>				
N2–H2···N7a	0.860	2.195	2.981	151.7
N4–H4···N7a	0.860	2.412	3.056	132.1
N4–H4···N5b	0.860	2.457	2.978	119.6
<b>2<sup>b</sup></b>				
N2–H2···N7a	0.860	2.231	2.988	146.8
N2–H2···N5	0.860	2.502	2.970	115.0
N4–H4···N5b	0.860	2.274	2.817	121.2
N4–H4···N7c	0.860	2.630	3.170	121.9
<b>3<sup>c</sup></b>				
N2–H2···O2	0.89	1.96	2.818	164
N4–H4···O2	0.92	1.86	2.780	174
C9–H9···O2c	0.96	2.33	3.276	169

<sup>a</sup> Symmetry code: *a* *x*,  $-y + 1/2$ ,  $z - 1/2$ ; *b*  $-x + 2$ ,  $-y + 1$ ,  $-z + 1$ .

<sup>b</sup> Symmetry code: *a*  $-x + 2$ ,  $y + 1/2$ ,  $-z + 3/2$ ; *b*  $-x + 2$ ,  $-y$ ,  $-z + 2$ ;  
*c* *x*,  $-y - 1/2$ ,  $z + 1/2$ . <sup>c</sup> Symmetry code: *c*  $0.5 - x$ ,  $1.5 - y$ ,  $1 - z$ .

seems quite unusual because the coordinating nitrogen (N3) atoms in this binding pattern have severe steric congestion because of the proximity of the methyl group to the metal ion. As a result, the binding mode of 5-methylpyrazole to the Co center is commonly encountered as exemplified in

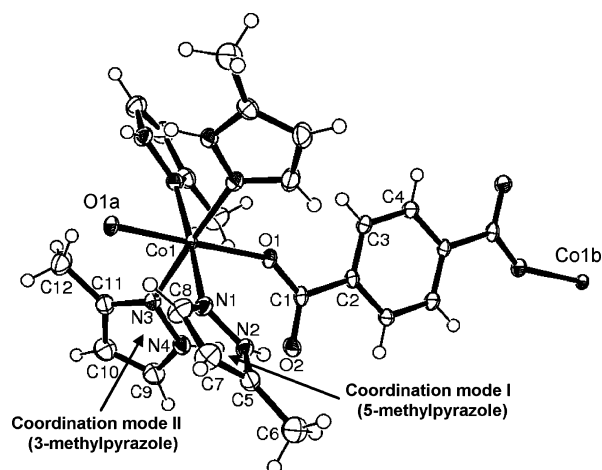


**Figure 4.** ORTEP representation of **3**. There are two coordination modes, 5-methylpyrazole, including the N1 atom, and 3-methylpyrazole, containing the N3 atom. Symmetry code: *a* =  $1 - x$ ,  $y$ ,  $1.5 - z$ ; *b* =  $-x$ ,  $y$ ,  $1.5 - z$ .

**Table 5.** Bond Lengths (Å) and Angles (deg) for **3**

Co(1)–O(1)	2.1106(15)	Co(1)–N(1)	2.144(2)
Co(1)–N(3)	2.155(2)		
O(1)–Co(1)–N(1)	91.78(7)	O(1)–Co(1)–N(3)	91.66(7)
N(1)–Co(1)–N(3)	92.06(7)	C(1)–O(1)–Co(1)	143.44(15)
C(8)–N(1)–Co(1)	129.49(16)	N(2)–N(1)–Co(1)	125.44(15)
C(11)–N(3)–Co(1)	135.50(16)	N(4)–N(3)–Co(1)	119.90(14)

the aforementioned mononuclear complexes. For instance, coordination polymers bridged by tp or azide ligands also exhibit the exclusive coordination pattern of 5-methylpyrazole, which explains the stability of 5-methylpyrazole relative to 3-methylpyrazole because of the structural hindrance.<sup>3</sup> These steric consequences are reflected on the bond distances between Co and the surrounding atoms, as the Co–N1 (5-methylpyrazole) bond length of 2.144(2) Å is shorter than the Co1–N3 (3-methylpyrazole) distance of 2.155(2) Å. The dihedral angle ( $\alpha$ ) between the carboxylate group and benzene ring of the tp ligand is 2.69(2)°, positioned on a lower end among the tp-bridged coordination compounds.<sup>3,8</sup> The tp ligand acts in a bis-monodentate manner, linking two Co atoms with the shortest Co···Co distance of 11.4804(2) Å, which is in the normal range for the tp bridge.<sup>3,8</sup>

The chain bridged by tp is also strengthened by the incorporation of hydrogen bonding. The intrachain hydrogen bonds are formed between the N–H groups of methylpyrazoles and free carboxylate oxygen atoms (N2···O2 = 2.818 Å; N4···O2 = 2.780 Å), as seen in Figure 5a. The chains are linked together through O2···H9–C9 (3-methylpyrazole) hydrogen bonding (C9···O2c = 3.276 Å, *c* =  $0.5 - x$ ,  $1.5 - y$ ,  $1 - z$ ), giving rise to an extended two-dimensional sheet (Figures 5b and S2). Such C–H···O hydrogen bonds are not observed in systems coordinated by 5-methylpyrazoles.<sup>3a,9</sup> Hence, the interchain hydrogen bonding, along with the intrachain hydrogen bonds, would likely promote the

(8) Cano, J.; De Munno, G.; Sanz, J. L.; Ruiz, R.; Faus, J.; Lloret, F.; Julve, M.; Caneschi, A. *J. Chem. Soc., Dalton Trans.* **1997**, 1915.

(9) Hong, C. S.; Yoon, J. H.; You, Y. S. *Inorg. Chim. Acta* **2005**, 358, 3341.

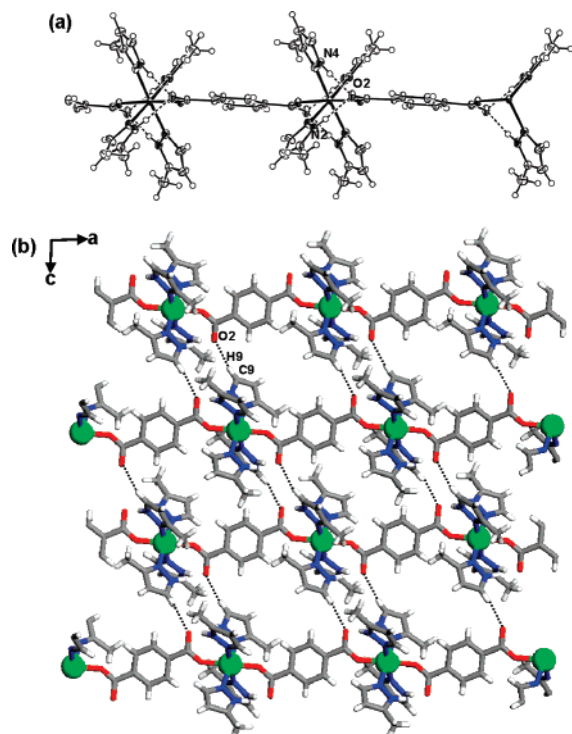


**Figure 5.** Extended view of **3** with (a) a one-dimensional chain bridged by tp and intrachain hydrogen bonds (dotted lines) and (b) a two-dimensional sheet showing C–H···O interchain hydrogen bonds (dotted lines) (C, gray; N, blue; O, red; Co, green).

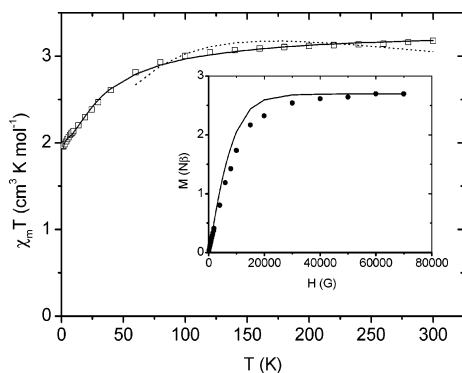


**Figure 6.** Plot of  $\chi_m T$  vs  $T$  for **3**. The magnetic data are fitted by the magnetic expression for an isolated hexacoordinated Co(II) ion including spin–orbit coupling and crystal-field parameters (dotted line) and the Rueff equation (solid line), respectively. The inset presents the field dependence of the magnetization at 1.8 K (●), and the solid line denotes the simulated curve by the Brillouin function.

stability of the relatively unstable 3-methylpyrazole in the crystal lattice. The shortest interchain Co–Co distance is 10.2449(2) Å.

**Magnetic Properties.** The magnetic susceptibility of **3**, shown in Figure 6, was measured in the temperature range of 1.8–300 K. When cooled, the  $\chi_m T$  value of 3.18 cm<sup>3</sup> K mol<sup>−1</sup> decreases slowly and then more rapidly at low temperatures, reaching a value of 1.96 cm<sup>3</sup> K mol<sup>−1</sup> at 1.8 K. To probe magnetic interactions between the Co(II) centers, the Curie–Weiss law was applied in the high-temperature range (60–300 K), affording  $C = 3.2$  cm<sup>3</sup> K mol<sup>−1</sup> and  $\theta = -9.1$  K. The Curie constant is in the usual range of octahedral high-spin Co(II) ions (2.8–3.4 cm<sup>3</sup> K mol<sup>−1</sup>).<sup>10–12</sup>

The overall diminution in  $\chi_m T$  with lowering temperature can be associated with antiferromagnetic interactions among magnetic centers or with spin–orbit coupling for Co(II) ions with a <sup>4</sup>T<sub>1g</sub> ground state in an octahedral field. The negative  $\theta$  value is correlated with a phenomenological consequence of the former antiferromagnetic interactions. To assess the latter effect, the magnetic data above 50 K were fitted by the expression for an isolated hexacoordinated Co(II) ion,<sup>13</sup> resulting in roughly estimated values of  $\lambda$  (spin–orbit coupling constant) of  $-91$  cm<sup>−1</sup>, consistent with the tp-bridged Co(II) dimer,<sup>8</sup> and  $A$  (crystal field parameter = 1.5 for the weak-field limit and 1.0 for the strong-field limit) values of 1.3.

Below 20–30 K a doubly degenerate level is only populated, and the Co spin may be characterized as an effective  $S = 1/2$  spin with a large  $g$  anisotropy.<sup>10</sup> The magnetization at 1.8 K is almost saturated above about 3 T, arriving at 2.69 N $\beta$  in 7 T, which is consistent with expected values for Co(II) (2–3 N $\beta$ ).<sup>10,11</sup> The Brillouin equation with  $S = 1/2$  and  $g = 5.38$  reproduces the saturation magnetization as depicted in the inset of Figure 6. The obtained  $g$  value is a reasonable one for octahedral Co(II) ions.<sup>10</sup> The experimental values in M(H) are lower than the calculated curve, demonstrating that antiferromagnetic interactions are operative. To obtain an estimated magnetic exchange coupling constant ( $J$ ) fit of the magnetic data with the Ising chain model at temperatures below 30 K was attempted and proved to be unsatisfactory.<sup>10,11</sup>

The contribution of antiferromagnetic interactions in the situation involved in spin–orbit coupling effect can be extracted by employing the Rueff expression<sup>12</sup>

$$\chi_m T = A \exp(-E_1/kT) + B \exp(-E_2/kT)$$

A best fit provides parameters of  $A + B = 3.3$  cm<sup>3</sup> K mol<sup>−1</sup>,  $E_1/k = 33.3$  K, and  $E_2/k = 0.15$  K. The value of  $A + B$  is close to the Curie constant (3.2 cm<sup>3</sup> K mol<sup>−1</sup>). The  $E_1/k$  value found, attributable to the spin–orbit coupling and site distortion effects, agrees well with those reported for one- and two-dimensional Co(II) systems.<sup>12,14</sup> The very weak interactions ( $-E_2/k = -0.15$  K) mediated by the long tp bridge are estimated to be  $J = -0.30$  K =  $-0.21$  cm<sup>−1</sup> in relation with the Ising chain approximation of  $\chi_m T \propto \exp(J/2kT)$ . The calculated  $J$  value is in good agreement with those of tp-bridged dinuclear and two-dimensional Co(II) complexes.<sup>8,14</sup>

## Conclusions

We have prepared two azide-bound M(II) [M = Mn(1), Ni(2)] monomers capped by 5-methylpyrazole, resulting in two-dimensional supramolecular assemblies formed by hy-

- (10) Carlin, R. L. *Magnetochemistry*; Springer-Verlag: Berlin, 1986.
- (11) Kahn, O. *Molecular Magnetism*; VCH: Weinheim, Germany, 1993.
- (12) (a) Rueff, J.-M.; Masciocchi, N.; Rabu, P.; Sironi, A.; Skoulios, A. *Eur. J. Inorg. Chem.* **2001**, 2843. (b) Rueff, J.-M.; Masciocchi, N.; Rabu, P.; Sironi, A.; Skoulios, A. *Chem.–Eur. J.* **2002**, *8*, 1813.
- (13) Raebiger, J. W.; Manson, J. L.; Sommer, R. D.; Geiser, U.; Rheingold, A. L.; Miller, J. S. *Inorg. Chem.* **2001**, *40*, 2578.
- (14) Manna, S. C.; Konar, S.; Zangrando, E.; Okamoto, K.-i.; Ribas, J.; Chaudhuri, N. R. *Eur. J. Inorg. Chem.* **2005**, 4646.

drogen bonds and  $\pi$ - $\pi$  contacts, and a tp-bridged Co(II) compound (**3**) with a two-dimensional sheet structure built by covalent and noncovalent bonds. For **3**, notably, the monodentate capping ligand methylpyrazole exhibits the coexistence of two coordination modes (5-methylpyrazole and 3-methylpyrazole) simultaneously to the same metal center. Special interests are in the unstable coordination mode, 3-methylpyrazole, that is stabilized by interchain C-H $\cdots$ O hydrogen bonds despite the steric hindrance. The effects of spin-orbit coupling and weak antiferromagnetic interactions in **3** are elucidated using the appropriate magnetic models.

**Acknowledgment.** This work was supported by the Korea Research Foundation Grant funded by the Korean Government (MOEHRD, Basic Research Promotion Fund) (KRF-2005-070-C00068) and CRM-KOSEF. C.S.H thanks an Operation Program on Shared Research Equipment of KBSI and MOST.

**Supporting Information Available:** Packing structures of **1** and **3** (Figures S1 and S2) and crystallographic information in CIF format. This material is available free of charge via the Internet at <http://pubs.acs.org>.

IC060429C